Published in Optics Communications 205, issues 4-6, 229-238, 2002
which should be used for any reference to this work

Measuring amplitude and phase distribution of fields generated by gratings with sub-wavelength resolution

A. Nesci*, R. Dändliker, M. Salt, H.P. Herzig

Institute of Microtechnology, University of Neuchâtel, Rue A..-L. Breguet 2, 2000 Neuchâtel, Switzerland

Abstract

In this paper, we intend to gain an understanding of the interaction of light with microstructures. Measurements of amplitude and phase in the diffracted field close to gratings using a heterodyne scanning probe are presented. Coherent light diffracted by microstructures produces periodic features and can give birth to phase dislocations, also called phase singularities. Phase singularities are isolated points where the amplitude of the field is zero. We present measurements of such phase singularities with 10 nm spatial sampling and compare them with theoretical results obtained from rigorous diffraction calculations. The observed polarization effects reveal also important information about the vectorial field conversion by the fiber tip.

1. Introduction

Measurements of amplitude $A(\vec{x})$ and phase $\phi(\vec{x})$ with a heterodyne scanning probe microscope [1–4] have been made in the optical field diffracted by periodic microstructures, in particular a holographically recorded 1 μm pitch grating. Most SNOM measurements are done at constant height (or constant intensity) in the X–Y plane (parallel to the surface) above the samples. However, the optical field diffracted by a structure depends strongly on the z-position, normal to the surface. Therefore, we have performed scans above the structures in the X–Z plane, perpendicular to the surface [5,6].

By illuminating the sample at normal incidence, we observe the diffracted field in transmission. In this case, we can investigate the propagation (in the z-direction) of the light after the periodic modulation, in both TE- and TM-polarization. The periodic reproduction of the optical features far behind the grating is explained by the *Talbot effect* [7]. The TM-mode contains x- and z-components (E_x and E_z) of the total electric field. The separation of the measured components of well-known fields can help us to understand the coupling of the field into the fiber tip and thus lead to a better interpretation of the image. Comparison with theoretical calculations using the Fourier modal method (FMM) shows good agreement with the amplitude and phase measurements.

We will show sub-wavelength measurements from a scanning probe optical microscope working at micrometer distances from a grating. One has to

* Corresponding author. Fax: +1-858-534-1225.
E-mail address: nesci@ece.ucsd.edu (A. Nesci).

differentiate the material object and the optical field. In general, the produced optical field is not equal to the geometrical shape of the object. Even if the size of the structure is larger than the wavelength, the optical features that are engendered are often smaller than the wavelength. A 10 nm lateral variation of the phase field can be achieved even without the contribution of evanescent waves. Using coherent detection (heterodyne), the optical field rather than the intensity is averaged by the tip, allowing the detection of phase singularities. Measurements of phase singularities are used to demonstrate sub-wavelength spatial resolution.

2. Diffraction by a grating

Let us consider the special case of a 1 μm pitch surface relief grating (Fig. 1). With a wavelength of $\lambda = 0.532$ μm, which is smaller than the pitch of $\Lambda = 1$ μm, we get for normal incidence three propagating wavevectors $\vec{k}_0$, $\vec{k}_{+1}$ and $\vec{k}_{-1}$. The diffraction angles (given by $\sin\theta = \lambda/\Lambda$) are $\theta_0 = 0°$ and $\theta_{\pm1} = 32.1°$. The orders $\vec{k}_{\pm m}$ for $m \geqslant 2$ are evanescent.

As the wavelength is smaller than the period of the grating, we will always get at least one propagating non-zero order. In this case, the evanescent orders are "hidden" by the diffracted orders in the far-field (at distances larger than λ). Two polarization states have to be distinguished. If the incident wave is linearly polarized and the electric field vector is perpendicular to the plane of incidence (X–Z plane), all diffracted orders have the same polarization, called s- or TE-polarization (Fig. 1(a)). The other case, where the electric wavevector is parallel to the incident plane, is called p- or TM-polarization (Fig. 1(b)). Any other polarization state can be expressed by a linear combination of these two fundamental states. In the TE case, only one component E_y of the electric vector is present, whereas in the TM case two components E_x and E_z have to be considered. Since E_x is perpendicular, but E_z parallel to the tip, the problem will be to know what is really detected by the SNOM tip: only E_x, or a combination of E_x and E_z? This is a crucial question, because the answer explains the behavior of the tip probe and might lead to know its transfer function [8–10] for the electrical field vector.

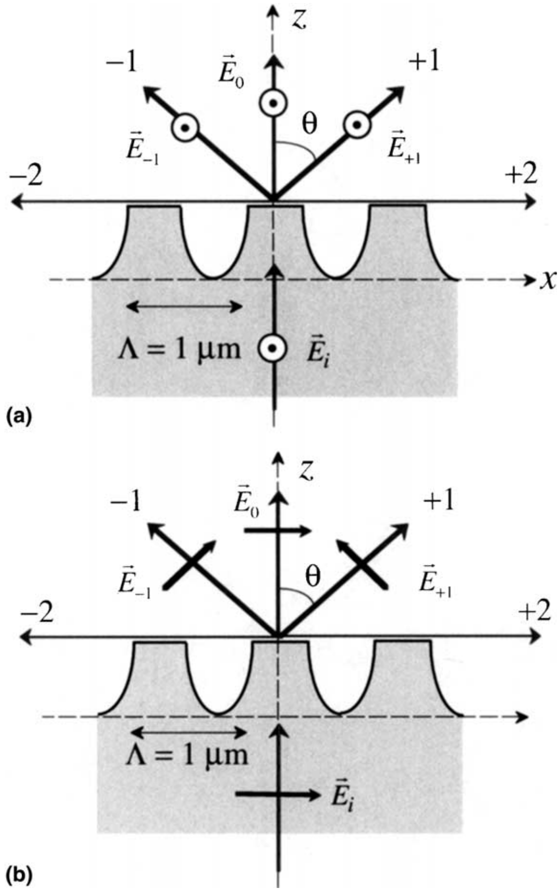

Fig. 1. Diffraction by a 1 μm pitch grating at normal incidence for: (a) TE-mode, and (b) TM-mode. Zero and first orders are propagating; the higher diffraction orders are evanescent.

3. Experimental setup

The illumination system for the sample is shown in Fig. 2(a). The light comes from a single-mode fiber and is collimated to get a plane wave. A half-wavelength plate rotates the polarization in order to get TE- or TM- polarization illumination. Then, the polarization is optimized with a Glan–Thomson polarizer. A 45°-mirror sends the light through the sample at normal incidence. The illumination

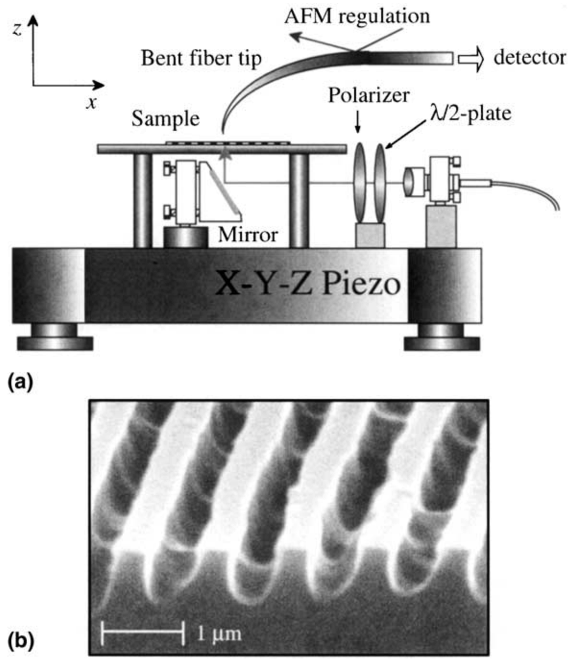

Fig. 2. (a) Experimental setup for the illumination of the sample and the fiber tip probe. The light beam reflected from the bent fiber is used to monitor the AFM contact mode (Park Scientific Instruments, Model Bioprobe). (b) SEM image of the holographically recorded 1 μm pitch grating in photo-resist. The depth is about 0.7 μm.

system and the sample are mounted on an x–y–z piezo-electric translation stage (100 μm × 100 μm × 20 μm range), which allows accurate translation steps (2 nm resolution in z-direction). The fiber tip is mounted independently from this translation system. The bent tip is used as a conventional atomic force microscope (AFM) cantilever [11] and is brought close to the surface. Once the tip approach is done, the AFM feedback (contact mode) is switched off and the scan (in XY or XZ planes) is accomplished by the x–y–z stage. The optical scanning probe microscope is combined with a heterodyne interferometer in order to get the phase information [4]. The light collected by the fiber probe is combined in a fiber coupler with a frequency shifted reference wave, producing the beat signal required for the heterodyne detection.

The sample is a 1 μm pitch quasi-binary shape grating recorded holographically in photo-resist. A scanning electron microscopy (SEM) picture of the grating is shown in Fig. 2(b). We use a dielectric fiber tip to collect the field information. The small coupling between the dielectric tip and the dielectric grating gives a negligible contribution to the total electric field [12]. Thus, the measured field should not be perturbed by the presence of the tip.

Usually, SNOM images are acquired in constant intensity or constant height mode (in the XY-plane) above the sample. However, in all SPM techniques, the absolute distance between the tip and the surface is not really known. Calculations predict periodic variations of the propagating field in the x- and z-directions. Indeed, the optical field depends strongly on the tip–surface distance. Therefore, we performed scans in the plane of incidence (X–Z) in order to see the propagation of the light (wavefronts) behind the sample.

4. TE-mode amplitude and phase measurement behind the grating

According to the setup of Fig. 2(a), measurements of the TE-mode amplitude (Fig. 3(a)) and phase (Fig. 3(b)) from a 1 μm pitch grating in the X–Z plane have been performed. The phase in Fig. 3(b) is represented by a contour plot (iso-phase lines). The distance between two "bold" lines is λ (and thus corresponds to 2π). The image has been acquired by scanning in the x-direction at constant height with a step of $\Delta x = 25$ nm, starting at $z = 10$ μm and moving down in $\Delta z = 50$ nm steps for further x-line scans. The total scan size is $x = 5$ μm by $z = 10$ μm and the number of pixels is 200×200. With a integration time of $\tau = 30$ ms, the global image is acquired in 20 min. The zero in the z-direction is arbitrary. The scan is executed until the tip touches the surface. There is excellent agreement with the theoretical expectations shown in Fig. 4. In Fig. 4(a), a discontinuity appears at the height $z = 0.4$ μm. At this position the tip touches the surface and damages the photo-resist structure. In the next section, this situation will be discussed in more detail.

In Fig. 3 we can see a periodic feature in the z-direction. A Fourier analysis of the diffracted field distribution explains this phenomenon, known as

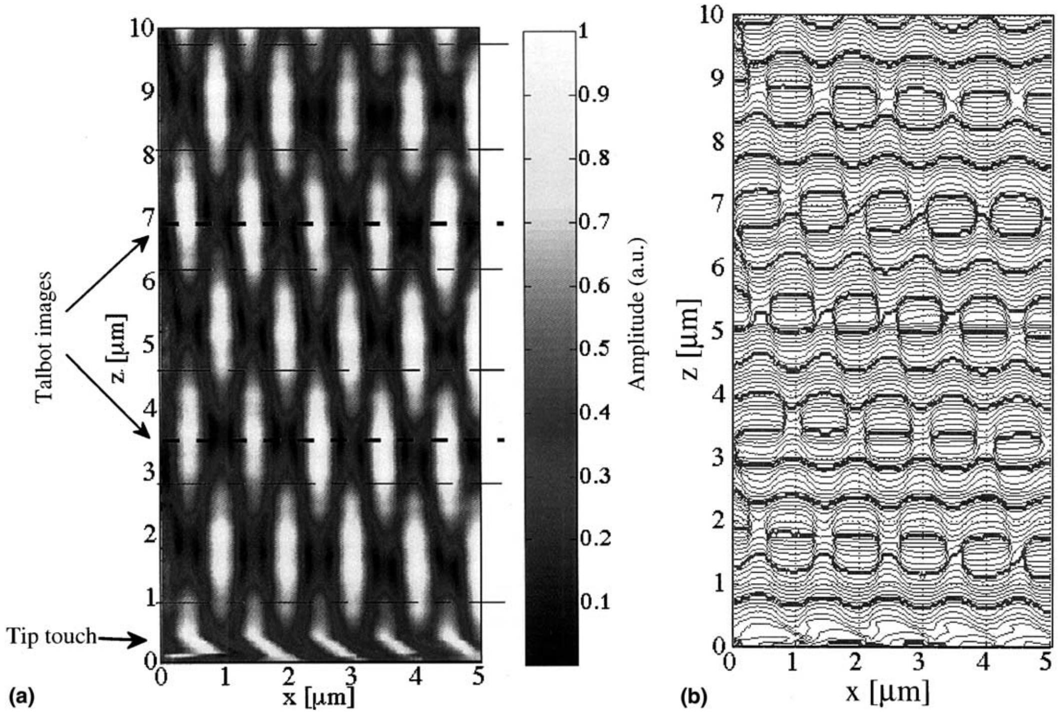

Fig. 3. Measured TE-mode optical field emerging from a 1 μm pitch grating (0.55 μm height): (a) normalized amplitude, and (b) contour plot of the phase (iso-phase lines). The scan size in the XZ plane is 5 μm in x-direction and 10 μm in z-direction (200 × 200 pixels). At $z = 0.4$ μm the tip touches the surface. The bold dashed lines are the Talbot images and the thin dashed lines are the Talbot subimages.

Talbot effect [7,13,14]. The intensity observed behind the grating at distances $z_m = 2m\Lambda^2/\lambda$, where m is an integer, is a reproduction of the intensity that would be observed just behind the grating [15]. Such images are called *Talbot images*. In our case, where $\Lambda_x = 1$ μm and $\lambda = 0.532$ μm, the Talbot planes are situated at $z_m = m \cdot 3.76$ μm (Fig. 3(a), with $m = 1, 2$). Talbot subimages with twice the frequency of the original grating ($\Lambda_x = 0.5$ μm) and reduced contrast are situated at distances $z_m = (m - 1/2)\Lambda^2\lambda^{-1}$, or $z_m = (m - 1/2) \cdot 1.88$ μm (thin dashed lines in Fig. 3(a)). The Talbot effect can be observed for any periodic structure.

5. Phase singularities produced by microstructures

A phase singularity, or a dislocation is an isolated point where the amplitude is zero [16]. At this point, the phase is not determined. Phase dislocations can be observed in the near- and far-field of optical microstructures, such as gratings [17]. The position of phase dislocations depends essentially on the period, the height, the shape and the fill-factor of the grating. Therefore, according to the position of the phase singularity, the structure of the grating can be recovered [18] by comparing the measured positions with rigorous calculations of the diffraction. However, the relationship between the position of the phase dislocation and the structure is not straightforward.

By zooming into a region of Fig. 3(b) (Fig. 4(b)), we can compare the measured phase distribution with the calculated one (Fig. 4(a)). Comparison with theoretical calculations using FMM leads us to the following observations [5]: from 0.5 μm above the grating, the measured phase agrees very well with the theory. Within the first 500 nm from

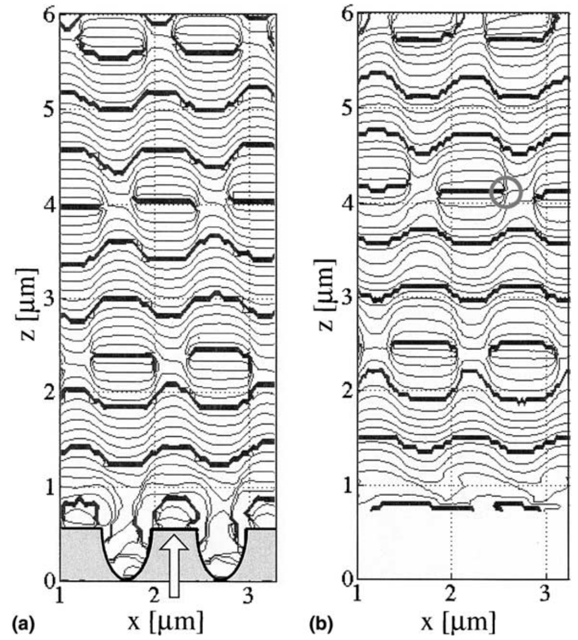

Fig. 4. Comparison of calculated and measured phase distributions for the grating: (a) Calculated phase distribution with the Fourier modal method, (b) measured phase (zoom from Fig. 3(b)). The circle encloses one phase singularity. The field within the first 500 nm from the top of the structure could not be measured, because the tip apex touched and damaged the grating. The zero of the z-position has been adapted to the absolute scale of the calculation.

the top of the structure, the field (amplitude and phase) is not correctly measured. Indeed, the tip apex touched the photo-resist surface before measuring the field closer to the structure. In fact, simulations for uncoated dielectric fiber tips show that the light is not captured at the apex of the tip, but rather at a distance of about 400–500 nm inside the tip. Measurements with coated tips give comparable results.

The evolution of the optical phase in time can be simulated by an additional linearly increasing phase of the reference wave. In Fig. 5 we present another measurement of the phase around a phase singularity using the following approach: the reference phase increases from Figs. 5(a)–(f) in steps of 60°. The spatial sampling of the measurements is 10 nm in the x-direction and 20 nm in the z-direction. We observe that the measured phase distribution changes its shape, but the phase singularity does not change its position. The phase distribution turns around the phase dislocation (which remains at a fixed position) as the wave propagates in z-direction.

Fig. 6 shows another measurement, but similar to a cross-section of Fig. 5(a) at $z = 1.18$ μm. By crossing the phase singularity, the amplitude makes a transition through zero (Fig. 6(a)) and the phase jump is always π (Fig. 6(b)). In this figure, we demonstrate that, at a phase singularity, the phase is not defined (because the signal vanishes in the noise) and the amplitude is really zero. In fact, we measured the zero amplitude, or more precisely, the zero optical power, down to $P_0 = 10^{-16}$ W (Fig. 6(a), with the marker "S"). The theoretical minimum detectable power at 50 Hz bandwidth is $P_0^{\min} = 2.7 \times 10^{-17}$ W, limited by the shot noise. Thus the detected point is very close to the shot noise. The transition of the phase in Fig. 6(b) is measured within one step of ±10 nm. The measured phase jump is as sharp as one step (with a slope of 18°/nm).

From these measurements we see that although the amplitude falls practically down to zero at the singularity, the signal-to-noise ratio around the phase singularity (Fig. 6(b), markers A and B, separated by 20 nm) is sufficiently large to locate the phase jump with high accuracy. In fact, in Fig. 6(b), the signal-to-noise ratios at the points A, S and B are $\mathrm{SNR_A} = 26$ dB, $\mathrm{SNR_S} = 6$ dB and $\mathrm{SNR_B} = 21$ dB, respectively, corresponding to the optical powers of $P_A = 10^{-14}$ W, $P_S = 10^{-16}$ W and $P_B = 3 \times 10^{-15}$ W. The resulting standard deviations for the phase measurement are $\delta\varphi_A = 3°$, $\delta\varphi_S = 30°$ and $\delta\phi_B = 5°$. Although the phase is not well measured at S, the transition is very well localized (within 10–20 nm) by the measurements at marks A and B in Fig. 6(b).

6. Polarization effects in TM-mode

In Section 4 we discussed the case of TE-mode diffraction by a grating. For the TM-mode the situation is more complicated, because the electric field has two components E_x and E_z. Therefore,

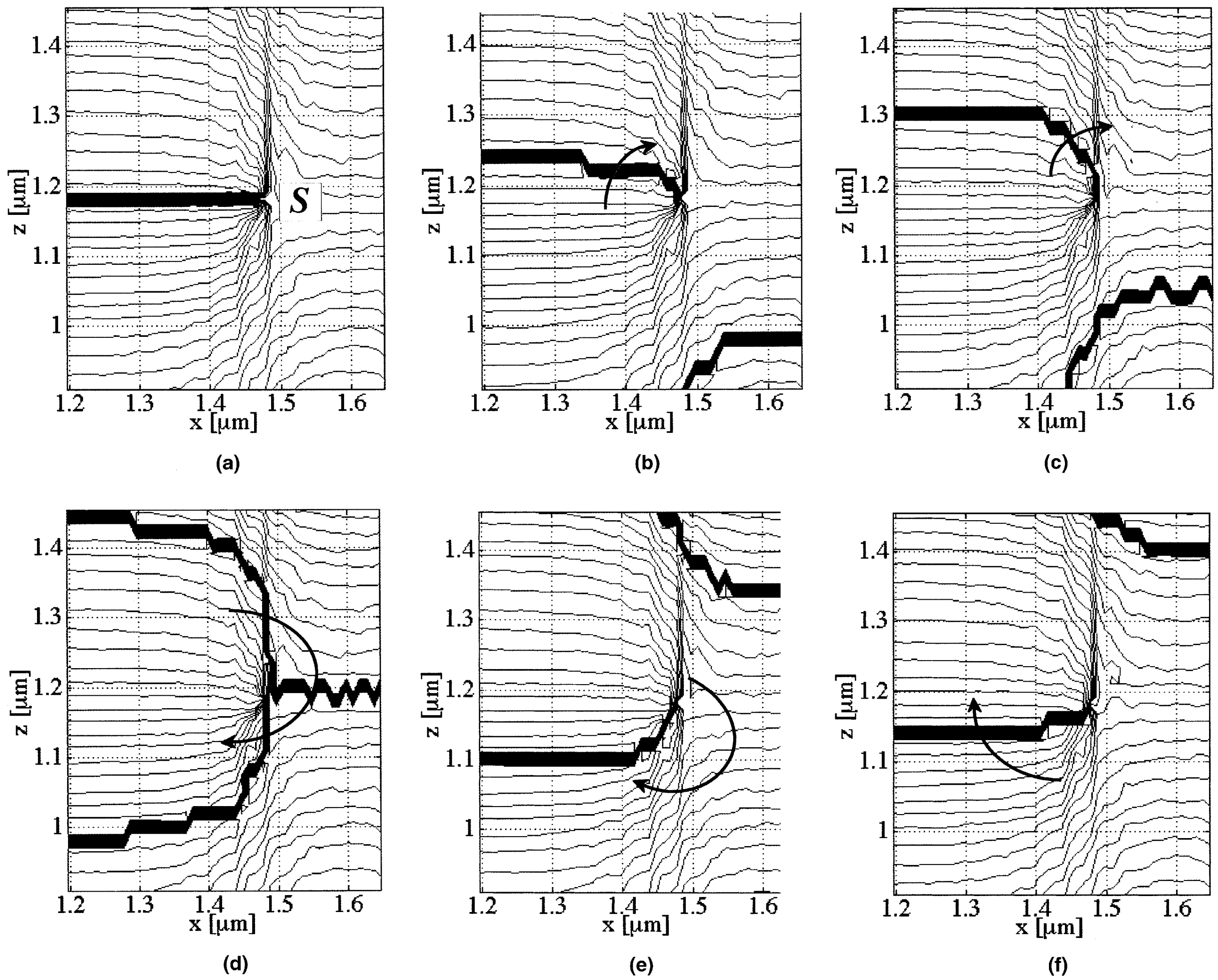

Fig. 5. Phase measurement around an isolated phase singularity ("S") located at $x = 1.48$ μm and $z = 1.18$ μm. The scan step is 10 nm in x-direction and 20 nm in the z-direction. The additional reference phase increases from (a) to (f) in steps of 60°. Two consecutives lines are separated by $\pi/10$.

the crucial question arises: what does the tip "see" and which field does it really capture? We will try to answer this fundamental question by analyzing the components of the diffracted field and by comparing the experimental results with the theoretical expectations. The measurements in the TM-mode have been performed with the same setup and under identical conditions as for the TE-mode. The results are shown in Fig. 7. Although the amplitude field may look quite similar to the TE-mode, we see that the phase is totally different.

For the TM-mode, the coupling of the two components of the diffracted total electric field E_x and E_z to the scanning probe has to be considered. For a single-mode 0°-cleaved fiber, only E_x would contribute to the fiber mode excitation. For a sharp fiber tip, the polarization coupling behavior is quite different and still not well established. The vector $\vec{E}$ is composed of the two orthogonal components E_x and E_z. Since they are orthogonal, they do not interfere. By introducing a fiber tip, the two components are coupled to the same propagating mode in the fiber [9,10] and can

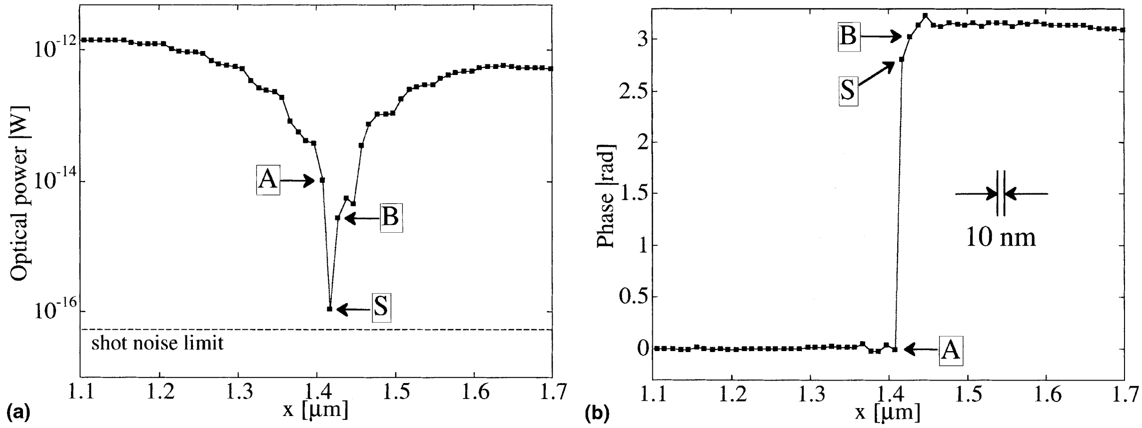

Fig. 6. Measured optical power and phase by crossing a phase singularity (S). The phase singularity is the special point where (a) the amplitude is zero, and (b) the phase jumps by π (with a quasi-infinite slope).

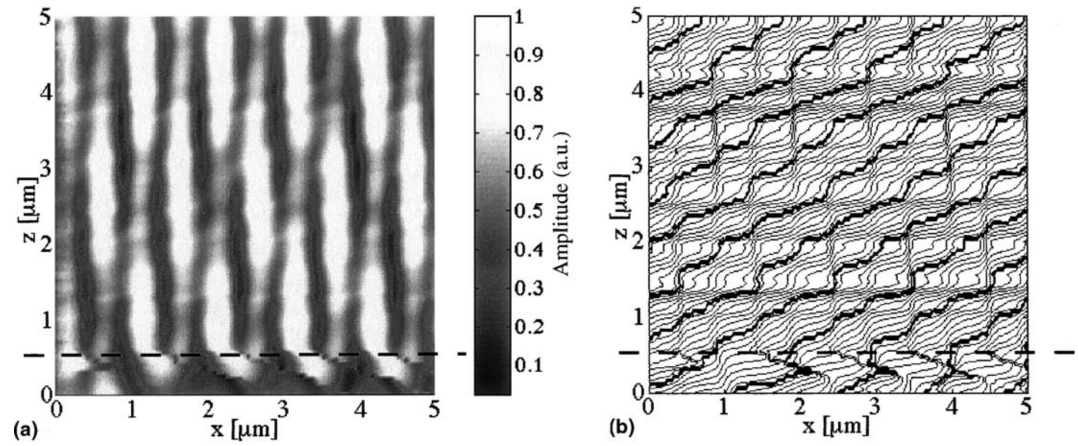

Fig. 7. Measured TM-mode diffraction of a 1 μm pitch grating (700 nm height): (a) amplitude, and (b) phase. At the position of $z = 0.58$ μm (dashed lines), the tip touches and damages the photo-resist structure.

therefore interfere with each another. This effect is similar to the interference of two orthogonal polarizations observed behind an analyzer, as explained in Fig. 8. By introducing the coupling coefficients [9] c_x and c_z, for the E_x and the E_z, component, respectively, we can express the total collected electric field by

$$E_{\text{coll}} = c_x E_x + c_z E_z. \tag{1}$$

In Fig. 9, we present the rigorous calculation of the diffracted field for each component E_x and E_z. in the TM-mode, using the FMM. For E_x, the diffracted field can be assimilated to the TE-mode by symmetry. For E_z, however, the behavior is completely different.

If we assume now that the coupling coefficients for E_x and E_z are the same ($c_x = c_z$), we get the amplitude and phase distribution of the collected field shown in Fig. 10. This result corresponds quite well with the measured distribution in Fig. 7. The analogy with the analyzer (Fig. 8) would correspond to a 45° orientation. It is interesting to note that the phase singularities have completely disappeared. It is important to be aware of this

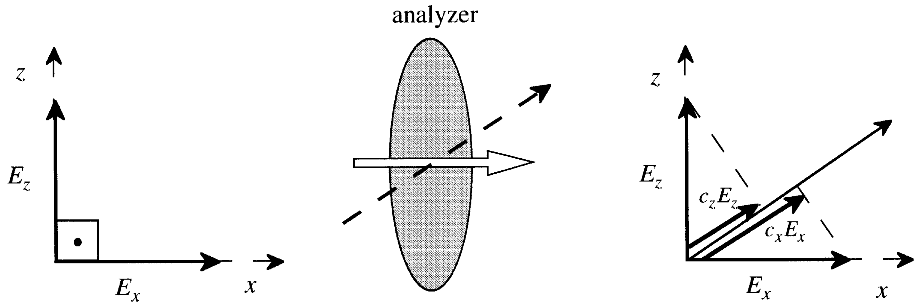

Fig. 8. Analyzer analogy of electric vector component coupling.

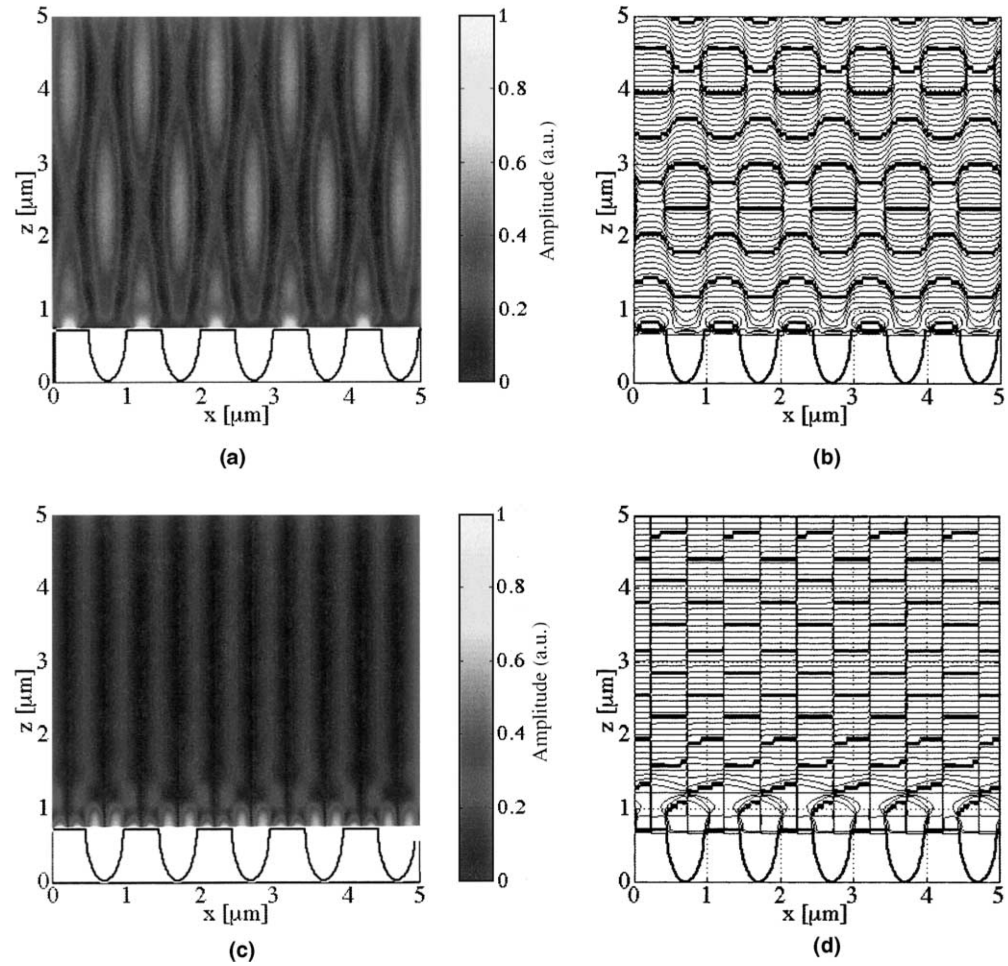

Fig. 9. Rigorously calculated field diffracted by a grating in the TM-mode. The field inside the structure is not presented. (a) Amplitude and (b) phase of the E_x component. (c) Amplitude and (d) phase of the E_z component.

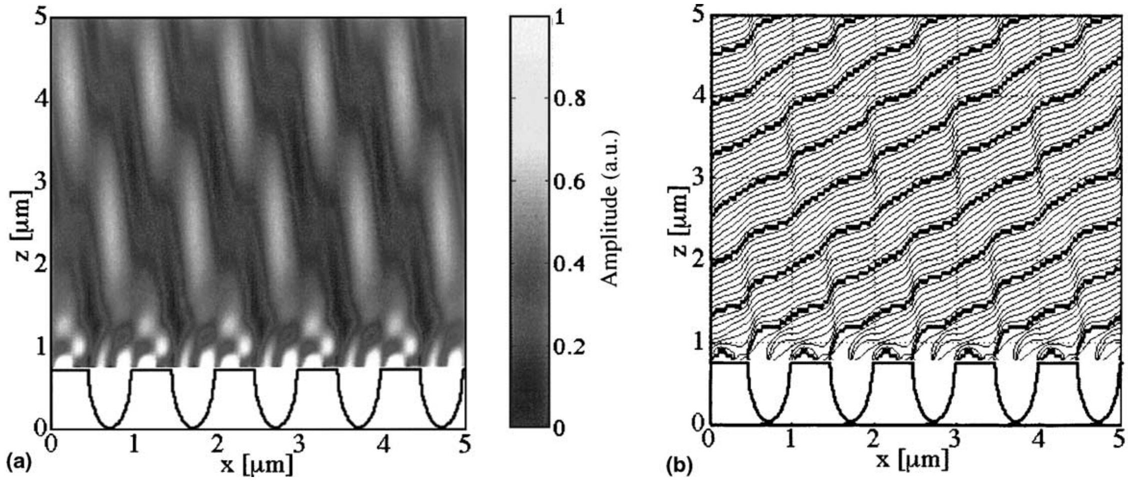

Fig. 10. Rigorously calculated (a) amplitude and (b) phase of the collected electric field for $c_x = c_z(E_{\rm coll} = E_x + E_z)$.

influence of the vector coupling behavior of the probe for image interpretation with scanning probe optical microscopes. The presented results demonstrate clearly that the phase distribution is more significant than the intensity (or amplitude squared) to establish the vector coupling properties of the probe and to avoid that artifacts are measured.

7. Conclusion

We have presented amplitude and phase measurements emerging from microstructures, in particular from gratings. The measurements have been made with a coherent heterodyne scanning probe optical microscope. Interaction with micro-optical structures changes the amplitude and phase of the incoming light field. Measuring the amplitude and the phase gives information about the structure, but the relationship is not trivial.

The properties of optical structures can be studied on the basis of phase singularities produced by the diffracted field. Although phase variations at these positions are very steep, they can be observed thanks to coherent detection with a scan step of 10 nm. The amplitude at phase dislocations is really zero (below the shot noise limit) and thus the signal-to-noise ratio vanishes, leaving the phase undefined. However, the signal-to-noise ratio of the measured points next to the phase transition is high enough, allowing the phase singularities to be localized with sub-wavelength accuracy.

The field conversion by a SNOM probe is not yet well understood. We tried to provide some answers to this mechanism by an analysis of the measured components of the electric field vector in TM-mode. Interesting polarization effects have been observed. Our conclusion is that the z-component of the diffracted field contributes nearly as much as the transverse x-component to the excitation of the propagating mode in the fiber probe. In the future, we hope that such studies will help to understand the field conversion, and thus to establish the vectorial transfer function of the tip.

Acknowledgements

This work has been supported by the Swiss National Science Foundation.

References

[1] A. Nesci, P. Blattner, H.P. Herzig, R. Dändliker, in: Nanoscale Optics, EOS Topical Meetings Digests Series Proceedings, vol. 25, European Optical Society, Paris, 2000, p. 52.

[2] M.L.M. Balistreri, J.P. Korterik, L. Kuipers, N.F. van Hulst, Phys. Rev. Lett. 85 (2000) 294.
[3] R. Hillenbrand, F. Keilmann, Phys. Rev. Lett. 85 (2000) 3029.
[4] A. Nesci, R. Dändliker, H.P. Herzig, Opt. Lett. 26 (2001) 208.
[5] A. Nesci, M. Salt, R. Dändliker, H.P. Herzig, in: SPIE's Annual Meeting 2001 Symposium, SPIE Proc. 4456 (2001) 68.
[6] A. Nesci, Measuring amplitude and phase in optical fields with sub-wavelength features, Thesis, University of Neuchâtel, Switzerland, 2001.
[7] H.F. Talbot, Philos. Mag. 9 (1836) 401.
[8] P. Blattner, H.P. Herzig, R. Dändliker, Opt. Commun. 155 (1998) 245.
[9] S.I. Bozhevolnyi, B. Vohnsen, E.A. Bozhevolnaya, Opt. Commun. 172 (1999) 171.
[10] J.J. Greffet, R. Carminati, Prog. Surf. Sci. 56 (1997) 133.
[11] K. Lieberman, A. Lewis, et al., Appl. Phys. Lett. 65 (1994) 648.
[12] J.-C. Weeber, F. de Fornel, J.P. Goudonnet, Opt. Commun. 126 (1996) 285.
[13] J.W. Goodman, in: Introduction to Fourier Optics, McGraw-Hill, New York, USA, 1996, p. 87.
[14] M.V. Berry, S. Klein, J. Mod. Opt. 43 (1996) 2139.
[15] I.I. Smolyaninov, C. Davis, Opt. Lett. 23 (1998) 1346.
[16] J.F. Nye, M.V. Berry, Proc. R. Soc. London A (1974) 165.
[17] P. Blattner, Light field emerging from periodic optical microstructures, Thesis, University of Neuchâtel, Switzerland, 1999.
[18] R. Dändliker, P. Blattner, C. Rockstuhl, H.P. Herzig, in: Singular Optics (optical vortices): Fundamentals and Applications, SPIE Proc. 4403 (2001) 257.